Available online at www.sciencedirect.com

SCIENCE DIRECT®

International Journal of Heat and Mass Transfer 48 (2005) 5205–5220

International Journal of HEAT and MASS TRANSFER

www.elsevier.com/locate/ijhmt

Condensation heat transfer and pressure drop of refrigerant R-410A flow in a vertical plate heat exchanger

W.S. Kuo [a], Y.M. Lie [a], Y.Y. Hsieh [b], T.F. Lin [a,*]

[a] Department of Mechanical Engineering, National Chiao Tung University, Hsinchu 30010, Taiwan, ROC
[b] Department of Mechanical Engineering, Nan Kai Institute of Technology, Nantou, Taiwan, ROC

Received 4 June 2005; received in revised form 30 July 2005
Available online 27 September 2005

Abstract

Heat transfer and associated frictional pressure drop in the condensing flow of the ozone friendly refrigerant R-410A in a vertical plate heat exchanger (PHE) are investigated experimentally in the present study. In the experiment two vertical counter flow channels are formed in the exchanger by three plates of commercial geometry with a corrugated sinusoidal shape of a chevron angle of 60°. Downflow of the condensing refrigerant R-410A in one channel releases heat to the upflow of cold water in the other channel. The effects of the refrigerant mass flux, imposed heat flux, system pressure (saturated temperature) and mean vapor quality of R-410A on the measured data are explored in detail. The results indicate that the R-410A condensation heat transfer coefficient and associated frictional pressure drop in the PHE increase almost linearly with the mean vapor quality, but the system pressure only exhibits rather slight effects. Furthermore, increases in the refrigerant mass flux and imposed heat flux result in better condensation heat transfer accompanying with a larger frictional pressure drop. Besides, the imposed heat flux exhibits stronger effects on the heat transfer coefficient and pressure drop than the refrigerant mass flux especially at low refrigerant vapor quality. The friction factor is found to be strongly influenced by the refrigerant mass flux and vapor quality, but is almost independent of the imposed heat flux and saturated pressure. Finally, an empirical correlation for the R-410A condensation heat transfer coefficient in the PHE is proposed. In addition, results for the friction factor are correlated against the Boiling number and equivalent Reynolds number of the two-phase condensing flow.

1. Introduction

Over the past decades among various hydrochlorofluorocarbon (HCFC) refrigerants, R-22 ($CHClF_2$) has been the most extensively used working fluid in air conditioning and refrigeration systems because of its excellent thermal properties. However, many evidences show the destruction of the ozone layer and the global warming problems related to R-22. This popular refrigerant will be phased out in a short period of time (before 2020) since the chlorine it contains has an ozone depletion potential (ODP) of 0.055 and comparatively high global warming potential (GWP) of 1500 based on the time horizons of 100 years [1,2]. As a result, the search for a replacement for R-22 has been intensified in recent years. The technical committee for the Alternative Refrigerants Evaluation Program (AREP) has proposed an updated list of the potential alternatives to R-22.

* Corresponding author. Tel.: +886 35 712121 55118; fax: +886 35 726 440.
E-mail address: tflin@mail.nctu.edu.tw (T.F. Lin).

0017-9310/$ - see front matter
doi:10.1016/j.ijheatmasstransfer.2005.07.023

Nomenclature

A	heat transfer area of the plate, m^2
b	channel spacing, m
Bo	Boiling number, dimensionless
Co	Convection number, dimensionless
c_p	specific heat, J/kg °C
D_h	hydraulic diameter, $D_h = 2b$, m
f	friction factor
Fr	Froude number, dimensionless
g	acceleration due to gravity, m/s^2
G	refrigerant mass flux, kg/m^2 s
G_{eq}	equivalent all liquid mass flux
h	heat transfer coefficient, W/m^2 °C
i_{fg}	enthalpy of vaporization, J/kg
k	conductivity, W/m °C
L	length from center of inlet port to center of exit port, m
LMTD	log mean temperature difference, °C
P	pressure, Pa
Pr	Prandtl number, dimensionless
Q	heat transfer rate, W
q	imposed heat flux, W/m^2
R_{wall}	thermal resistance of the wall
Re_l	Reynolds number, $Re_l = \frac{G \cdot D_h}{\mu_l}$, dimensionless
Re_{eq}	equivalent all liquid Reynolds number, dimensionless
T	temperature, °C
U	overall heat transfer coefficient, W/m^2 °C
u	velocity, m/s
v	specific volume, m^3/kg
W	mass flow rate, kg/s
X	vapor quality

Greek symbols

ΔP	pressure drop
ΔX	total quality change in the exchanger
ρ	density, kg/m^3
μ	viscosity, Ns/m^2

Subscripts

ave	average
de	deceleration
ele	elevation
exp	experiment
f	frictional
fg	difference between liquid phase and vapor phase
g	vapor phase
i, o	at inlet and exit of test section
l	liquid phase
m	average value for the two phase mixture or between the inlet and exit
man	the test section inlet and exit manifolds and ports
p	preheater
r	refrigerant
tp	two phase
w	water
wall	wall/fluid near the wall

Some of the alternatives on the AREP's list are R-410A, R-410B, R-407C and R-507. Among these alternatives to R-22, refrigerant R-410A is the most widely used zero ODP refrigerant and is currently recognized as the main replacement to R-22. It is a mixture of R-32 and R-125 (50% by mass) which exhibits azeotropic behavior with a small temperature glide of about 0.1 °C. In order to properly use these new refrigerants, we need to know their thermodynamic, thermophysical, transport and heat transfer properties. Specifically, the detailed heat transfer characteristics of the condensation and boiling heat transfer and associated frictional pressure drops are very important in the design of heat exchangers used in many refrigeration and air conditioning systems. The main purpose of this study is to investigate the condensation heat transfer and associated frictional pressure drop for refrigerant R-410A in a vertical plate heat exchanger.

Several studies have been reported in the open literatures on the condensation heat transfer for refrigerant R-22 flow in various enhanced tubes, especially the micro-fin tubes [3–6], and the results were compared with those for refrigerant R-134a. In the following the relevant literature on the forced convective condensation heat transfer for R-410A is briefly reviewed. Sami and Poirier [7] compared the evaporation and condensation heat transfer data for several refrigerant blends proposed as substitutes for R-22, including R-410A, R-410B, R-507 and the quaternary mixture R-32/125/143a/134a inside enhanced-surface tubings. They showed that the two-phase heat transfer coefficients and pressure drops increased with the refrigerant mass flux for all refrigerants tested. The condensation heat transfer coefficients for R-410A, R-407C and R-22 flowing inside a horizontal smooth tube measured by Ebisu and Torikoshi [8] indicated that the condensation heat transfer coefficient of R-410A was slightly lower than that of R-22. Moreover, the R-410A condensation pressure drop was about 30% lower than that for R-22. The quantitative differences in the pressure drops between R-410A and R-22 were mainly attributed to the differences in vapor density of two refrigerants. Similar study was carried out by Wijaya and Spatz [9] for refrigerants R-22 and R-410A in a horizontal smooth copper tube. They indicated that the condensation heat transfer coefficients for R-410A were slightly higher than those for R-22, while the R-410A pressure drops were significantly lower than those for R-22. Condensation heat transfer and pressure drop of R-410A and R-22 inside a herringbone-type micro-fin tube examined by Miyara et al. [10] showed that both the condensation heat transfer coefficient and pressure drop for R-410A and R-22 in the herringbone-type micro-fin tube were higher than that in the helical micro-fin tube in the higher mass velocity region. For smooth horizontal tubes Chitti and Anand [11] showed that R-410A had about 15–20% higher regionally averaged condensation heat transfer coefficient when compared to R-22 at a given refrigerant mass flux rate. In a continuing study [12,13], Guo and Anand examined the condensation of R-410A in a rectangular channel focusing on the measurement and prediction of condensation heat transfer coefficients and on the relationship between the heat transfer coefficient and two-phase flow regimes. Besides, the R-410A condensation heat transfer coefficient was found to decrease with decreases in local quality and refrigerant mass flux.

It is well known that plate heat exchangers (PHEs) have been extensively used in food processing, chemical reaction processes and many other industrial applications for many years due to their effectiveness, compactness, flexibility, cost competitiveness, and the accessibility of the heat-exchanger surface. Although they are used primarily for liquid-to-liquid heat transfer, their performance is also good in boiling and condensation applications. Therefore, they have been introduced to the refrigeration and air conditioning systems as evaporators or condensers. The basic construction, plate patterns, flow arrangements, advantages and limitations of PHEs were clearly described by Shah and Focke [14]. Analyses of flow pattern in PHE to give some local information on the heat transfer and velocity field were carried out by Thonon et al. [15]. Besides, they proposed the heat transfer coefficient and pressure drop correlations for two-phase flows in PHE based on the models originally developed for smooth tubes. Tribbe, Müller-Steinhagen and their colleague [16–18] recently measured pressure drop for steady adiabatic gas/liquid flow in a single channel of a plate frame heat exchanger. Their results indicated that the pressure drop was greatly influenced by the channel geometry and it increased linearly with the flow quality.

In view of the scarcity in the two-phase heat transfer data for PHEs, Lin and his colleagues [19–23] recently carried out a series of experiments to investigate the evaporation, condensation, saturated and subcooled flow boiling of refrigerant R-134a and R-410A in a vertical plate heat exchanger. Specifically, they [19,20] experimentally measured the evaporation and condensation heat transfer coefficients and frictional pressure drops for R-134a in a vertical PHE. They showed that the evaporation heat transfer for R-134a flowing in the PHE was much better than that in circular tubes, particularly in high vapor quality convection dominated regime. Both the heat transfer coefficient and pressure drop increased with the imposed heat flux, refrigerant mass flux and vapor quality. Furthermore, it was noted that at a higher system pressure the heat transfer coefficients were slightly lower. Moreover, the rise in the heat transfer coefficient with the vapor quality was larger than that in the pressure drop. Hsieh and Lin [21] investigated the saturated flow boiling heat transfer and associated pressure drop for R-410A in the PHE. Their data manifested that the saturated boiling heat transfer coefficient and pressure drop in the PHE increased almost linearly with the imposed heat flux and the effects of the R-410A mass flux on the heat transfer coefficient were significant at a high imposed heat flux. Later, they [22] measured the subcooled flow boiling heat transfer of R-134a in the PHE. They also inspected the associated bubble characteristics such as bubble generation frequency and bubble size by visualizing the boiling flow. Finally, the measured data for the evaporation of R-410A in the PHE [23] indicated that both the evaporation heat transfer coefficient and frictional pressure drop increased with the refrigerant mass flux at low vapor quality. In addition, raising the imposed heat flux was noted to significantly improve the evaporation heat transfer. However, the friction factor is insensitive to the imposed heat flux and refrigerant pressure.

The above literature review clearly reveals that although R-410A is one of the most possible substitutes for R-22, the boiling and condensation heat transfer data for R-410A are still very scarce. To complement our previous studies on the two-phase heat transfer of R-134a and R-410A in the plate heat exchanger [19–23], the condensation heat transfer and associated pressure drop characteristics of refrigerant R-410A in a vertical plate heat exchanger are experimentally investigated in this study.

2. Experimental apparatus and procedures

The experimental apparatus established in the present study, as schematically shown in Fig. 1, to investigate the condensation heat transfer and associated frictional pressure drop of refrigerant R-410A in a vertical PHE consists of four independent loops and a data acquisition system. It includes a refrigerant loop, two water loops (one for preheater and another for the test section), and a cold water–glycol loop. Refrigerant R-410A is circulated in the refrigerant loop. To obtain various test conditions of R-410A (including the imposed heat flux, refrigerant mass flux, system pressure and inlet vapor quality) in the test section, we need to control the temperature and flow rate in the other three loops.

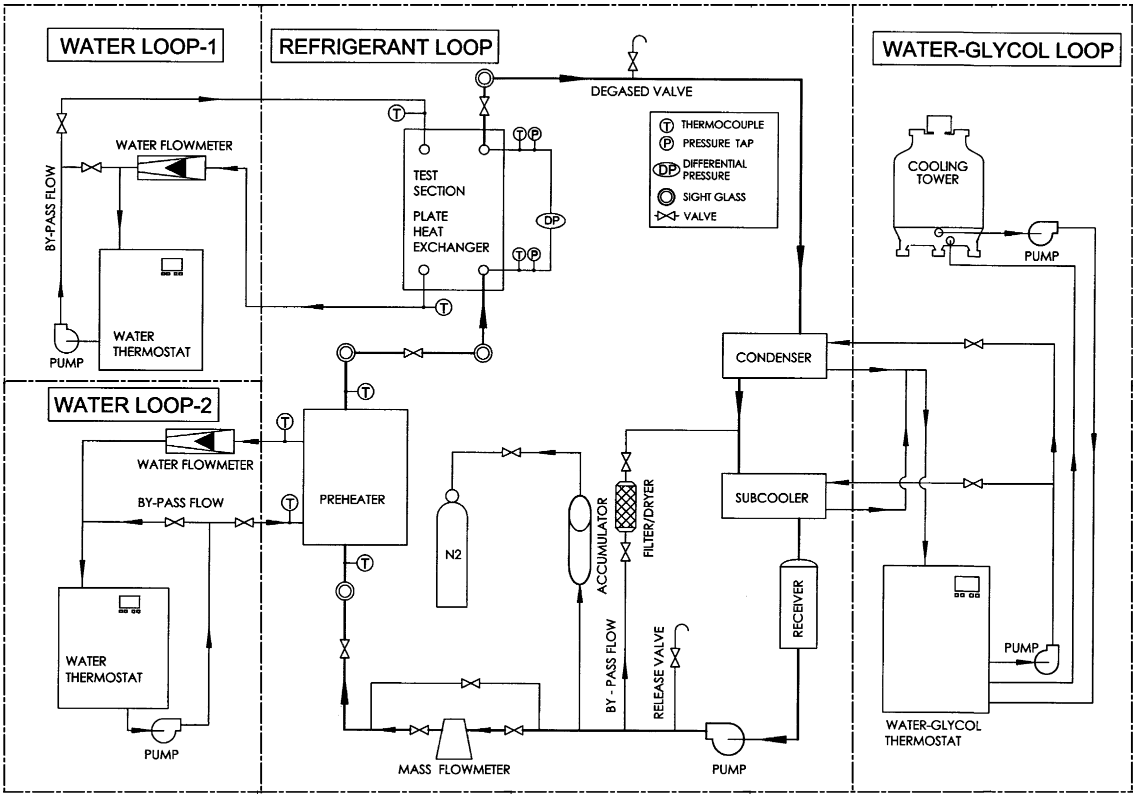

Fig. 1. Schematic diagram of the experimental system.

2.1. Refrigerant flow loop

The refrigerant loop contains a variable-speed refrigerant pump that delivers the subcooled refrigerant to the preheater. The refrigerant mass flow rate is mainly controlled by an AC motor through the change of the inverter frequency. The flow rate can be further adjusted by regulating the bypass valve in the flow path from the refrigerant pump. To measure the refrigerant mass flow rate, an accurate mass flux meter (Micromotion, model DS12S-100SU) is installed between the refrigerant pump and preheater with a reading accuracy of ±1%. The preheater is used to evaporate the subcooled liquid refrigerant R-410A to a specified vapor quality at the test section inlet by receiving heat from the hot water in the water loop. Finally, the vapor–liquid refrigerant mixture leaving the test section is condensed and subcooled by the low temperature water–glycol in the shell-and-coil heat exchangers acting as condenser and subcooler. An accumulator is connected to a high-pressure nitrogen tank to dampen the fluctuations of the flow rate and pressure. In addition, the loop also equips with a receiver, a filter/dryer, a release valve, a degassed valve and four sight glasses. The pressure of the refrigerant loop can be controlled by varying the temperature and flow rate of the water–glycol in the condenser and subcooler. Two absolute pressure transducers are installed at the inlet and exit of the test section with resolution up to ±2 kPa. Furthermore, a calibrated differential pressure transducer is used to measure the overall pressure drop across the refrigerant side of the vertical PHE. All the water and refrigerant temperatures are measured by Type T (copper–constantan) thermocouples with a calibrated accuracy of ±0.2 °C. A polyethylene insulation layer of 5-cm thick is wrapped around the whole loop to reduce the heat loss to the ambient.

2.2. Plate heat exchanger

Three commercial SS-316 plates manufactured by the Kaori Heat Treatment Co. Ltd., Taiwan, form the plate heat exchanger for the R-410A condensation heat transfer test. The plate surfaces are pressed to become grooved with a corrugated sinusoidal shape and 60° of chevron angle, which is the angle of V-grooves to the vertical axis of the plate. The detailed configuration for the plate heat exchanger is illustrated schematically in Fig. 2. The corrugated grooves on the right and left outer plates have a V shape but those in the middle plate

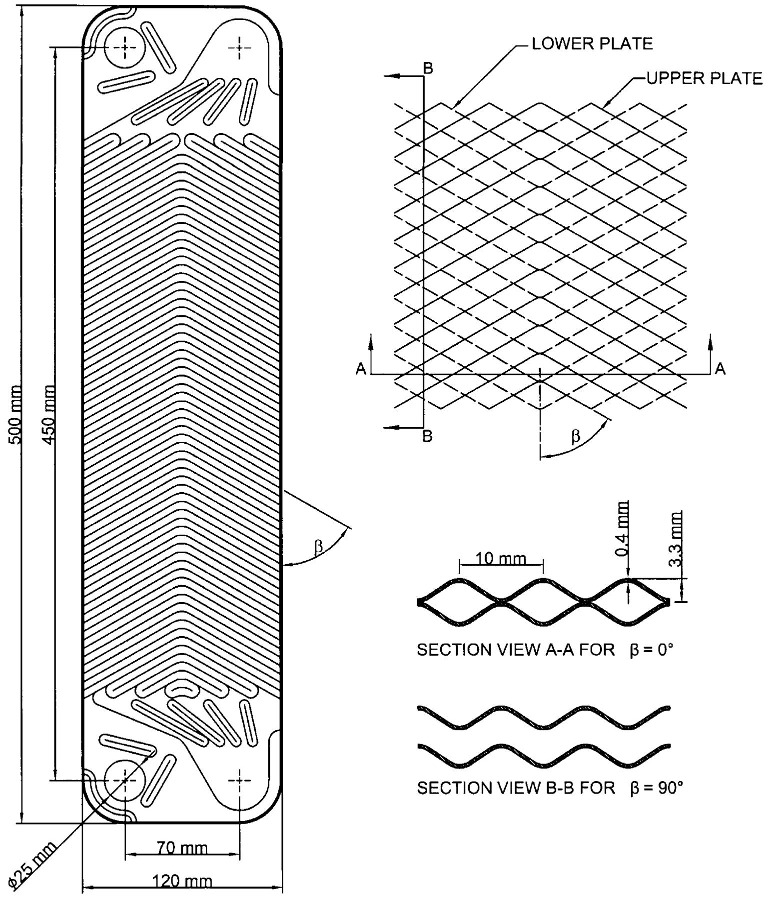

Fig. 2. Schematic diagram of the plate.

have a contrary V shape on both sides. This arrangement allows the flow stream to be divided into two different flow directions along the plates. Thus, the flow moves mainly along the grooves in each plate. Due to the contrary V shapes between two neighbor plates the flow streams near the two plates cross each other in each channel. This cross flow streams result in significant flow unsteadiness and randomness. In fact, the flow is highly turbulent even when the Reynolds number is low. In the plate heat exchanger three plates form two vertical counter flow channels. Downflow of refrigerant R-410A in one channel releases heat to the upflow of the cold water in the other channel. The heat transfer rate in the test section is calculated by measuring the total temperature rise and the flow rate in the water channel.

2.3. Water loop for test section

The water loop for the test section in the experimental system circulates the cold water through the test section. It contains a 40-l water thermostat with a 2.25-kW heater and an air cooled refrigeration system of 2.25-kW cooling capacity intending to control the water temperature. A 0.5-hp water pump is used to drive the cold water through the test section at a specified water flow rate. To obtain the desired imposed heat flux in test section, a by-pass valve can also be used to adjust the water flow rate. The accuracy of measuring the water flow rate is ±0.5%.

2.4. Water loop for preheater

Another water loop designed for the preheater consists of a 125-l hot water thermostat and a water pump which drives the hot water at specified temperature and flow rate to the preheater. Similarly, a by-pass valve is also used to adjust the flow rate.

2.5. Water–glycol loop

Both the condenser and subcooler, which respectively condense and subcool the refrigerant R-410A leaving the test section, are cooled by an independent low-temperature water–glycol loop. The cooling capacity is

3.5 kW for the water–glycol at −20 °C. A 0.5-hp pump is used to drive the water–glycol at a specified flow rate to the condenser as well as to the subcooler. A by-pass valve is also provided to adjust the flow rate.

2.6. Data acquisition

The data acquisition system includes a recorder (Yokogawa HR-2300), a 24 V–3 A power supply, and a controller. The water flowmeter and differential pressure transducer need the power supply as a driver to output an electric current of 4–20 mA. The data signals are collected and converted by a data acquisition unit (Hybrid recorder). The converted signals are then transmitted to a host computer through a GPIB interface for further calculation.

2.7. Experimental procedures

In each test the system pressure at the test section is first maintained at a specified level by adjusting the water–glycol temperature and flow rate through the condenser and subcooler. Then, the vapor quality of R-410A at the test section inlet is kept at the desired value by adjusting the temperature and flow rate of the hot water loop in the preheater. Next, the heat transfer rate between the counterflow channels in the test section can be varied by changing the water temperature and flow-rate in the water loop for the test section. Meanwhile, by selecting the frequency of the inverter connecting to the refrigerant pump and by adjusting the by-pass valve, the R-410A mass flow rate in the test section is maintained at a desired value.

During the test any changes of the system variables will lead to fluctuations in the temperature and pressure of the refrigerant flow. It takes about 20–100 min for the system to reach a statistically stable state at which variations of the time-average inlet and outlet temperatures are both less than ±0.2 °C, and the variations of the pressure and imposed heat flux are within 1% and 4%, respectively. Then the data acquisition system is initiated to scan all the data channels for ten times in 50 s. The mean value of the data for each channel is used to calculate the condensation heat transfer coefficient and associated frictional pressure drop. Additionally, the flow rate of water in the test section should be high enough to have turbulent flow in the water side so that the associated single-phase heat transfer in it is high enough for balancing the condensation heat transfer in the refrigerant side.

Before examining the R-410A condensation heat transfer characteristics, a preliminary test for single-phase water-to-water convective heat transfer in the vertical plate heat exchanger is performed. The Wilson's method [24] is adopted to calculate the relation between the single-phase heat transfer coefficient and the flow rate from these data. The single-phase heat transfer coefficient can then be used to analyze the data acquired from the condensation heat transfer experiments.

Table 1
Summary of the uncertainty analysis

Parameters	Uncertainty	
	Absolute value	Relative value (%)
PHE geometry		
Length, width and thickness	$\pm 5\times10^{-3}$ m	±1.5
Area of the plate	$\pm 7\times10^{-5}$ m^2	±2.0
Sensors		
Temperature, T	±0.2 °C	±3
Temperature difference, ΔT	±0.2 °C	±4.5
System pressure, P	±200 Pa	±1
Differential pressure, ΔP	±200 Pa	±1.5
Water flow rate, W	±0.02 kg/s	±2
Mass flux of refrigerant, G	±2 kg/m^2 s	±2
Condensation heat transfer		
Average vapor quality, X_m	±0.05	±8
Boiling heat flux, q	±1.5 kW/m^2	±6.5
Heat transfer coefficient, h_r	±300 W/m^2 °C	±17.5
Frictional pressure drop, ΔP_f	±650 Pa	±16.8
Friction factor, f_{tp}	±0.35	±16.5

2.8. Uncertainty analysis

The uncertainties of the experimental results are analyzed by the procedures proposed by Kline and McClintock [25]. The detailed results from the present uncertainty analysis for the experiments conducted here are summarized in Table 1.

3. Data reduction

The reduction of the data for the single-phase convection heat transfer coefficient in the vertical plate heat exchanger has been performed by Hsieh and Lin [21].

The reduction procedures for the condensation heat transfer coefficient from the raw data measured here are described in the following. Firstly, the total heat transfer rate between the counter flows in the PHE is calculated from the cold water side,

$$Q_w = W_w \cdot c_{p,w} \cdot (T_{w,o} - T_{w,i}) \tag{1}$$

Then, the refrigerant vapor quality at the test section inlet is evaluated from the energy balance for the preheater. Based on the measured temperature drop and flow rate on the water side, the heat transfer in the preheater is calculated from the relation

$$Q_{w,p} = W_{w,p} \cdot c_{p,w} \cdot (T_{w,p,i} - T_{w,p,o}) \tag{2}$$

The heat transfer from the water to the refrigerant in the preheater results in the rise of the refrigerant temperature to the saturated state (sensible heat transfer) and in the evaporation of the refrigerant (latent heat transfer). Thus

$$Q_{\mathrm{w,p}} = W_{\mathrm{r}} \cdot c_{p,\mathrm{r}} \cdot (T_{\mathrm{r,p,o}} - T_{\mathrm{r,p,i}}) + W_{\mathrm{r}} \cdot i_{\mathrm{fg}} \cdot X_{\mathrm{p,o}} \tag{3}$$

The above two equations can be combined to evaluate the refrigerant quality at the exit of the preheater, that is considered to be the same as the vapor quality of the refrigerant entering the test section. Specifically,

$$X_{\mathrm{i}} = X_{\mathrm{p,o}} = \frac{1}{i_{\mathrm{fg}}} \cdot \left[\frac{Q_{\mathrm{w,p}}}{W_{\mathrm{r}}} - c_{p,\mathrm{r}} \cdot (T_{\mathrm{r,p,o}} - T_{\mathrm{r,p,i}})\right] \tag{4}$$

The change in the refrigerant vapor quality in the test section is then deduced from the heat transfer to the refrigerant in the test section,

$$\Delta X = \frac{Q_{\mathrm{w}}}{W_{\mathrm{r}} \cdot i_{\mathrm{fg}}} \tag{5}$$

The overall heat transfer coefficient U between the two counter channel flows can be expressed as

$$U = \frac{Q_{\mathrm{w}}}{A \cdot \mathrm{LMTD}} \tag{6}$$

here the log-mean temperature difference (LMTD) is determined from the relation

$$\mathrm{LMTD} = \frac{((T_{\mathrm{r,o}} - T_{\mathrm{w,i}}) - (T_{\mathrm{r,i}} - T_{\mathrm{w,o}}))}{\ln\left[\frac{(T_{\mathrm{r,o}} - T_{\mathrm{w,i}})}{(T_{\mathrm{r,i}} - T_{\mathrm{w,o}})}\right]} \tag{7}$$

with $T_{\mathrm{r,i}}$ and $T_{\mathrm{r,o}}$ being the saturated temperatures of R-410A corresponding respectively to the inlet and outlet pressures in the refrigerant flow in the PHE. Finally, the condensation heat transfer coefficient in the flow of R-410A is evaluated from the equation

$$h_{\mathrm{r}} = \frac{1}{\left(\frac{1}{U}\right) - \left(\frac{1}{h_{\mathrm{w}}}\right) - R_{\mathrm{wall}} \cdot A} \tag{8}$$

where h_{w} is calculated from the single-phase water-to-water heat transfer test.

To evaluate the friction factor associated with the R-410A condensation in the refrigerant channel in the vertical PHE, the frictional pressure drop ΔP_{f} is calculated by subtracting the pressure losses at the test section inlet and exit manifolds and ports ΔP_{man}, and by adding the deceleration pressure rise during the R-410A condensation ΔP_{de} and the elevation pressure rise ΔP_{ele} from the measured total pressure drop ΔP_{exp} in the refrigerant channel,

$$\Delta P_{\mathrm{f}} = \Delta P_{\mathrm{exp}} - \Delta P_{\mathrm{man}} + \Delta P_{\mathrm{de}} + \Delta P_{\mathrm{ele}} \tag{9}$$

The deceleration and elevation pressure rises are estimated by the homogeneous model for two-phase gas–liquid flow [26],

$$\Delta P_{\mathrm{de}} = G^2 \cdot v_{\mathrm{fg}} \cdot \Delta X \tag{10}$$

$$\Delta P_{\mathrm{ele}} = \frac{g \cdot L}{v_{\mathrm{m}}} \tag{11}$$

where v_{m} is the mean specific volume of the vapor–liquid mixture in the refrigerant channel when the vapor and liquid are homogeneously mixed and is given as

$$v_{\mathrm{m}} = [X_{\mathrm{m}} \cdot v_{\mathrm{g}} + (1 - X_{\mathrm{m}}) \cdot v_{\mathrm{l}}] = [v_{\mathrm{l}} + X_{\mathrm{m}} \cdot v_{\mathrm{fg}}] \tag{12}$$

The pressure drop in the inlet and outlet manifolds and ports was empirically suggested by Shah and Focke [14]. It is approximately 1.5 times the head due to flow expansion at the test section inlet

$$\Delta P_{\mathrm{man}} \cong 1.5 \cdot \left(\frac{u_{\mathrm{m}}^2}{2v_{\mathrm{m}}}\right)_{\mathrm{i}} \tag{13}$$

where u_{m} is the mean flow velocity. With the homogenous model the mean velocity is

$$u_{\mathrm{m}} = G \cdot v_{\mathrm{m}} \tag{14}$$

Based on the above estimation, the deceleration pressure rise and the pressure losses at the test section inlet and exit manifolds and ports are found to be rather small. In fact, the summation of ΔP_{de} and ΔP_{man} ranges from 1% to 3% of the total pressure drop. According to the definition

$$f_{\mathrm{tp}} = -\frac{\Delta P_{\mathrm{f}} \cdot D_{\mathrm{h}}}{2G^2 \cdot v_{\mathrm{m}} \cdot L} \tag{15}$$

the friction factor for the condensation heat transfer of refrigerant R-410A in the PHE is obtained.

4. Results and discussion

In the present study of R-410A condensation heat transfer in the vertical plate heat exchanger, the condensation temperature of R-410A is varied from 20.0 °C to 31.5 °C (saturated pressure from 1.44 MPa to 1.95 MPa) for the refrigerant mass flux and imposed heat flux respectively ranging from 50 kg/m^2 s to 150 kg/m^2 s and from 5 kW/m^2 to 20 kW/m^2. In what follows the measured condensation heat transfer coefficient and frictional pressure drop are presented in terms of their variations with the mean vapor quality in the test section. Moreover, comparisons of the present data for R-410A with those for R-134a in the same PHE from Yan et al. [20] and with the results for R-410A in a smooth pipe from Ebisu and Torikoshi [8] and Wijaya and Spatz [9] are also conducted. Finally, correlation equations for the present data are proposed.

4.1. Condensation heat transfer

Effects of the refrigerant mass flux, imposed heat flux and system pressure (refrigerant saturated temperature) on the R-410A condensation heat transfer in the PHE are now inspected. Selected measured data are presented in Fig. 3 to illustrate the changes of the condensation heat transfer coefficient with the mean vapor quality in the test section for various flow and thermal conditions.

The effects of the refrigerant mass flux are illustrated first in Fig. 3(a) by presenting the variations of the measured condensation heat transfer coefficient with the mean vapor quality at the saturated pressure of 1.44 MPa ($T_{sat} = 20$ °C) and imposed heat flux of 10 kW/m^2 for the refrigerant mass flux ranging from 50 kg/m^2 s to 150 kg/m^2 s and the mean vapor quality varying from 0.10 to 0.80. In the plots X_m denotes the average vapor quality in the PHE estimated from X_i and ΔX. These results indicate that at given refrigerant mass flux, imposed heat flux and system pressure, the R-410A condensation heat transfer coefficient increases almost linearly with the mean vapor quality of the refrigerant in the PHE. This increase is rather significant. Specifically, a large increase in h_r with X_m is noted for a high refrigerant mass flux ($G = 150$ kg/m^2 s). For instance, at $P = 1.44$ MPa, $q = 10$ kW/m^2 and $G = 150$ kg/m^2 s the condensation heat transfer coefficient at the mean vapor quality of 0.80 is about 55% larger than that at $X_m = 0.10$. This obviously results from the simple fact that in the higher vapor quality regime the vapor and liquid shear stresses on the plate surface are much larger, meanwhile the liquid film is relatively thin. This, in turn, reduces the resistance of heat transfer from the plate surface to the refrigerant.

The results in Fig. 3(a) also demonstrate that a rise in the refrigerant mass flux always produces a significant increase in the condensation heat transfer coefficient at high vapor quality mainly due to the convective effect. High convective effect is caused by the high vapor quality and high refrigerant mass flux. In the low vapor quality regime ($X_m < 0.30$) the condensation heat transfer coefficient is only slightly affected by the refrigerant mass flux. As the mean vapor quality exceeds 0.4, the condensation heat transfer coefficient affected by the mass flux is clearly noted. Besides, for the higher G the heat transfer coefficient rises with the vapor quality more quickly than that for the lower mass flux. For example, the condensation heat transfer enhances by a factor of 1.1 for G raised from 50 to 150 kg/m^2 s at $X_m = 0.10$. However at $X_m = 0.80$ the enhancement factor is increased to 1.5. This is conjectured that at the high vapor quality and high refrigerant mass flux, the void fraction of the refrigerant is very high and the vapor flow moves turbulently at a high speed, which in turn results in a substantial rise in the condensation heat transfer coefficient in the PHE.

Next, the condensation heat transfer affected by the imposed heat flux is shown in Fig. 3(b) by presenting the variations of the heat transfer data with the mean vapor quality for three heat fluxes of 10, 15 and 20 kW/m^2 at $G = 100$ kg/m^2 s and $P = 1.44$ MPa. Note that the condensation heat transfer coefficient increases apparently with the imposed heat flux. Compared with the refrigerant mass flux effects shown in Fig. 3(a), the imposed heat flux exhibits a slightly stronger effect on

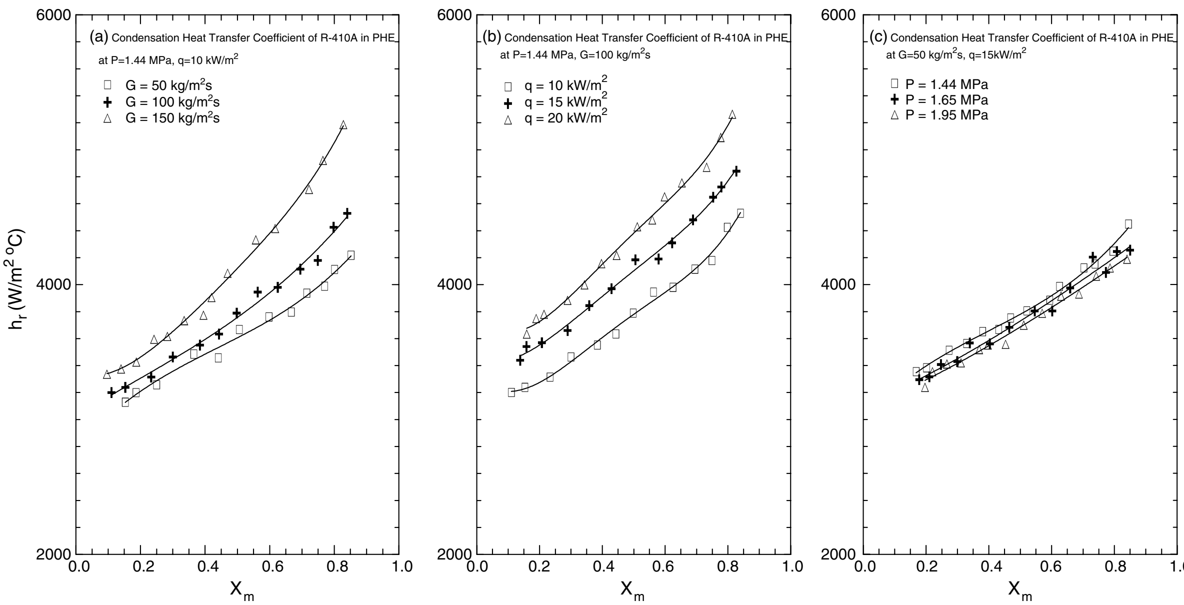

Fig. 3. Variations of condensation heat transfer coefficient with mean vapor quality for various refrigerant mass fluxes (a), imposed heat fluxes (b), and system pressures (c).

the condensation heat transfer coefficient over the entire range of the vapor quality tested here.

Then, how the refrigerant saturated pressure affects the R-410A condensation heat transfer coefficient is exemplified in Fig. 3(c) by presenting the data at $q = 15\ \mathrm{kW/m^2}$ and $G = 50\ \mathrm{kg/m^2\ s}$ at different saturated pressures for $P = 1.44$, 1.65 and 1.95 MPa which respectively correspond to the saturated temperatures of 20 °C, 25 °C and 31.5 °C for refrigerant R-410A. The results indicate that an increase in the system pressure leads to a rather slight change in the condensation heat transfer coefficient.

Finally, in Fig. 4 we compare the present data for the R-410A condensation heat transfer coefficient with those for R-134a in the same PHE reported by Yan et al. [20] and with those for R-410A in a horizontal smooth pipe

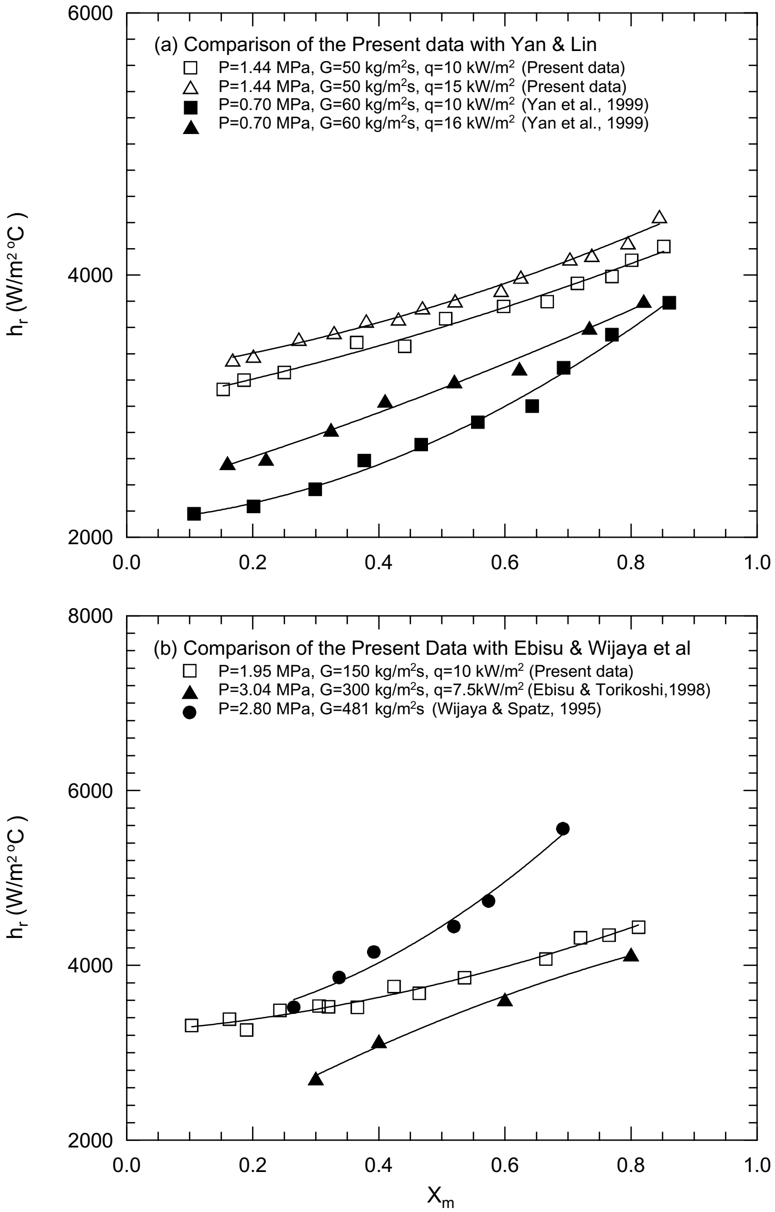

Fig. 4. Comparison of the measured R-410A condensation heat transfer coefficients for PHE with those for (a) R-134a in the same PHE from Yan et al. (1999) and (b) R-410A in a horizontal smooth tube from Ebisu and Torikoshi (1998) and from Wijaya and Spatz (1995).

measured by Ebisu and Torikoshi [8] and by Wijaya and Spatz [9]. The results in Fig. 4(a) manifest that both the condensation heat transfer coefficients for R-410A and R-134a in the PHE increase almost linearly with the mean vapor quality. Besides, the quality-averaged condensation heat transfer coefficient for R-410A is about 20–30% higher than that for R-134a. However, the condensation heat transfer coefficient for R-134a increases faster with the mean vapor quality than that for R-410A. The difference is attributed mainly to the different thermal conductivities of two refrigerants for the liquid and vapor phases. Specifically, the liquid thermal conductivity of R-410A is higher than that for R-134a by about 20%. However, the vapor thermal conductivity for R-410A is lower than that for R-134a. Hence, at lower quality the condensation heat transfer coefficient for R-410A is significantly higher than that for R-134a. The comparison given in Fig. 4(b) further indicates that for R-410A the condensation heat transfer coefficient in the PHE is higher than that in a horizontal smooth tube from Ebisu and Torikoshi [8]. This enhanced condensation is mainly attributed to the plate

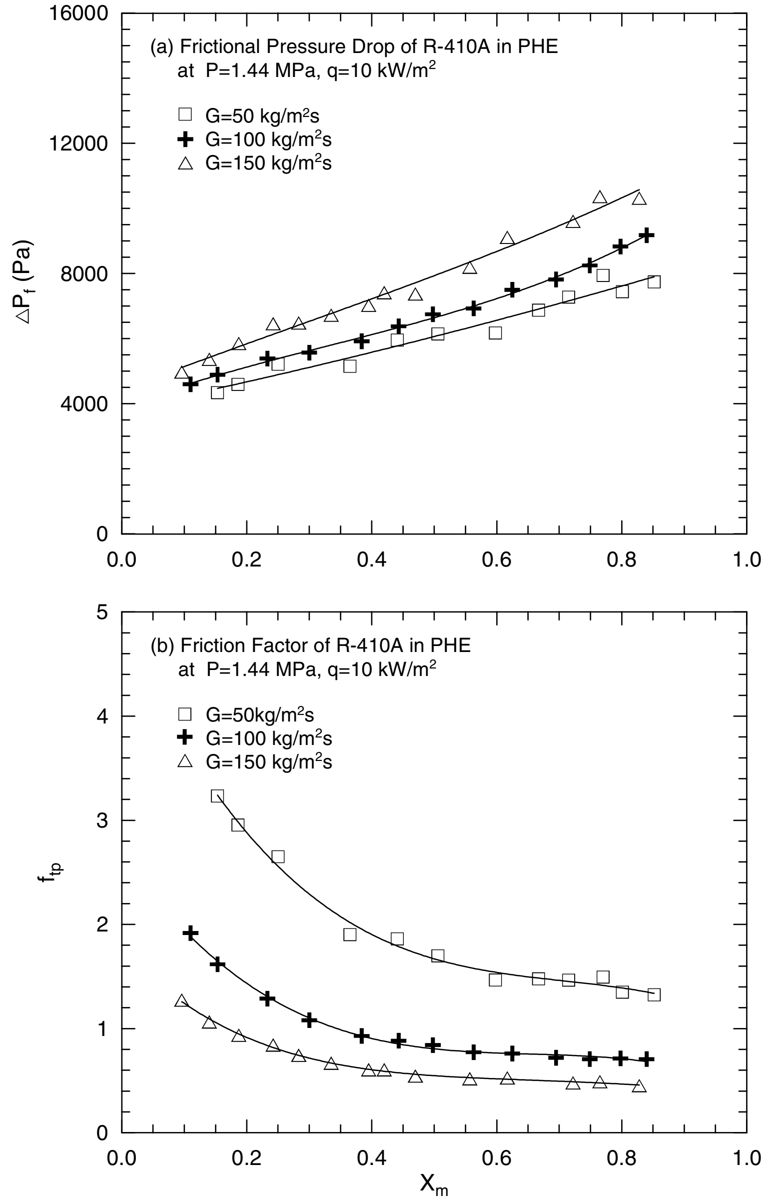

Fig. 5. Effects of refrigerant mass flux on (a) frictional pressure drop and (b) friction factor at $P = 1.44$ MPa and $q = 10$ kW/m^2.

surface corrugation and swirl flow generated in the PHE. However, our condensation heat transfer coefficient is lower than that reported by Wijaya and Spatz [9]. This is simply due to the fact that the refrigerant mass flux for the present data is only about 1/5 of their measurement [9].

4.2. Two-phase frictional pressure drop

The frictional pressure drop and friction factor associated with the refrigerant R-410A condensation in the vertical plate heat exchanger for various flow and thermal conditions are presented in Figs. 5–7. Besides, comparisons of the present data in the vertical PHE with those of R-134a in the same PHE and with those of R-410A in horizontal smooth tubes are shown in Fig. 8.

The results for ΔP_f given in Fig. 5(a) for different R-410A refrigerant mass fluxes indicate that at a given G the frictional pressure drop increases almost linearly with the mean vapor quality, similar to the results for the condensation heat transfer coefficient shown in Fig. 3(a). In addition, the pressure drop is noticeably

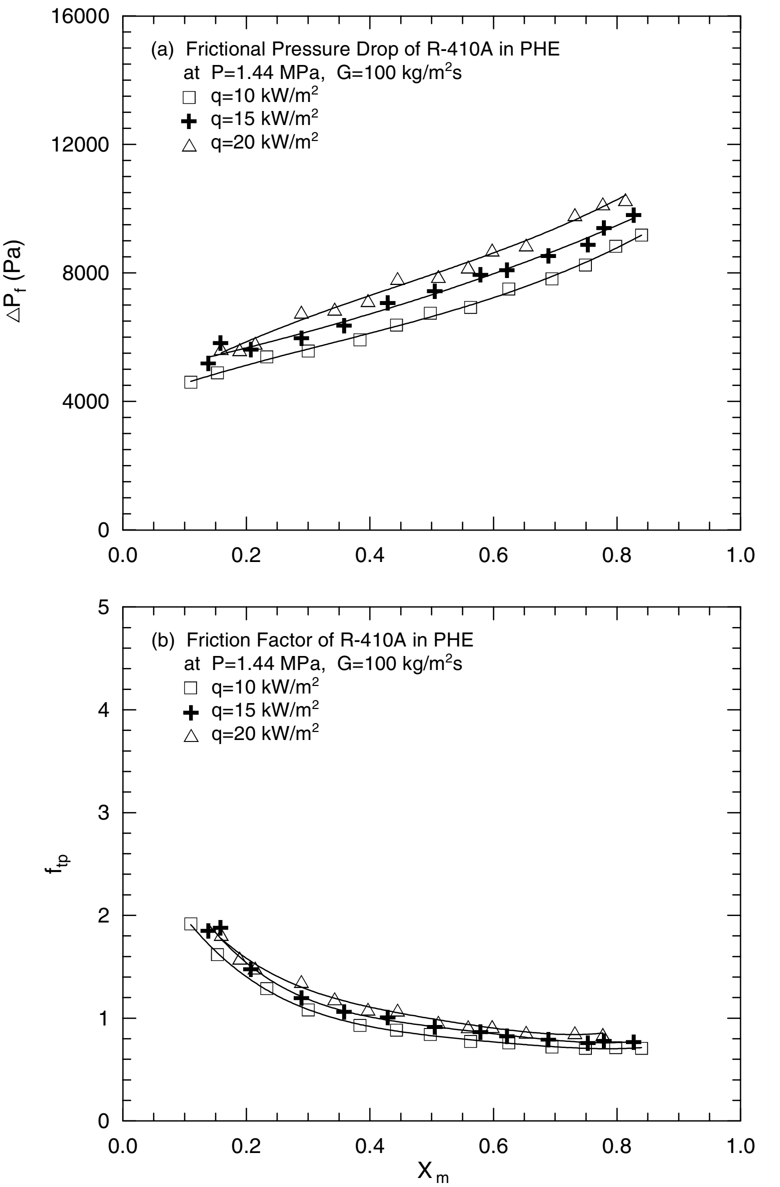

Fig. 6. Effects of imposed heat flux on (a) frictional pressure drop and (b) friction factor at $P = 1.44$ MPa and $G = 100$ kg/m^2 s.

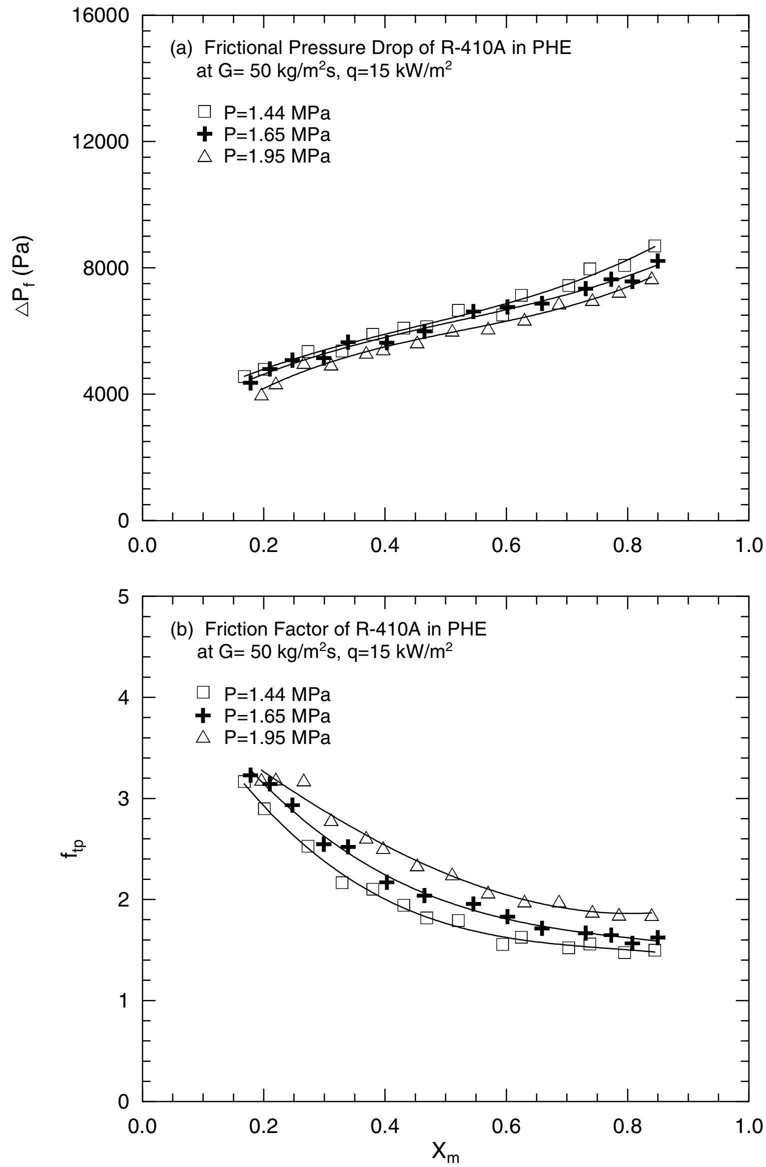

Fig. 7. Effects of refrigerant saturated pressure on (a) frictional pressure drop and (b) friction factor at $G = 50\ \mathrm{kg/m^2\ s}$ and $q = 15\ \mathrm{kW/m^2}$.

higher for a higher mass flux. For instance, for the refrigerant mass flux of $G = 150\ \mathrm{kg/m^2\ s}$ the frictional pressure drop is about 20% and 31% on average higher than those for $G = 100$ and $50\ \mathrm{kg/m^2\ s}$, respectively. Fig. 5(b) presents the variations of the friction factor with the mean vapor quality. The results manifest that the friction factor decreases exponentially with the mean vapor quality. This is conjectured to result from the fact that at the low vapor quality, the mean specific volume of the vapor–liquid mixture is low, which in turn results in a higher friction factor, according to Eq. (15). Moreover, the friction factor is lower at a higher refrigerant mass flux. This simply reflects the definition of the friction factor given in Eq. (15) that f_{tp} is proportional to G^{-2}. Next, the data in Fig. 6(a) suggest that an increase in the imposed heat flux results in a small rise in the frictional pressure drop. The effect of the imposed heat flux on the friction factor shown in Fig. 6(b) exhibits a similar trend. We further note that the two-phase frictional pressure drop is only slightly affected by the system pressure (Fig. 7). Finally, the data in Fig. 8 show that in the high vapor quality regime ($X_m > 0.4$), the frictional pres-

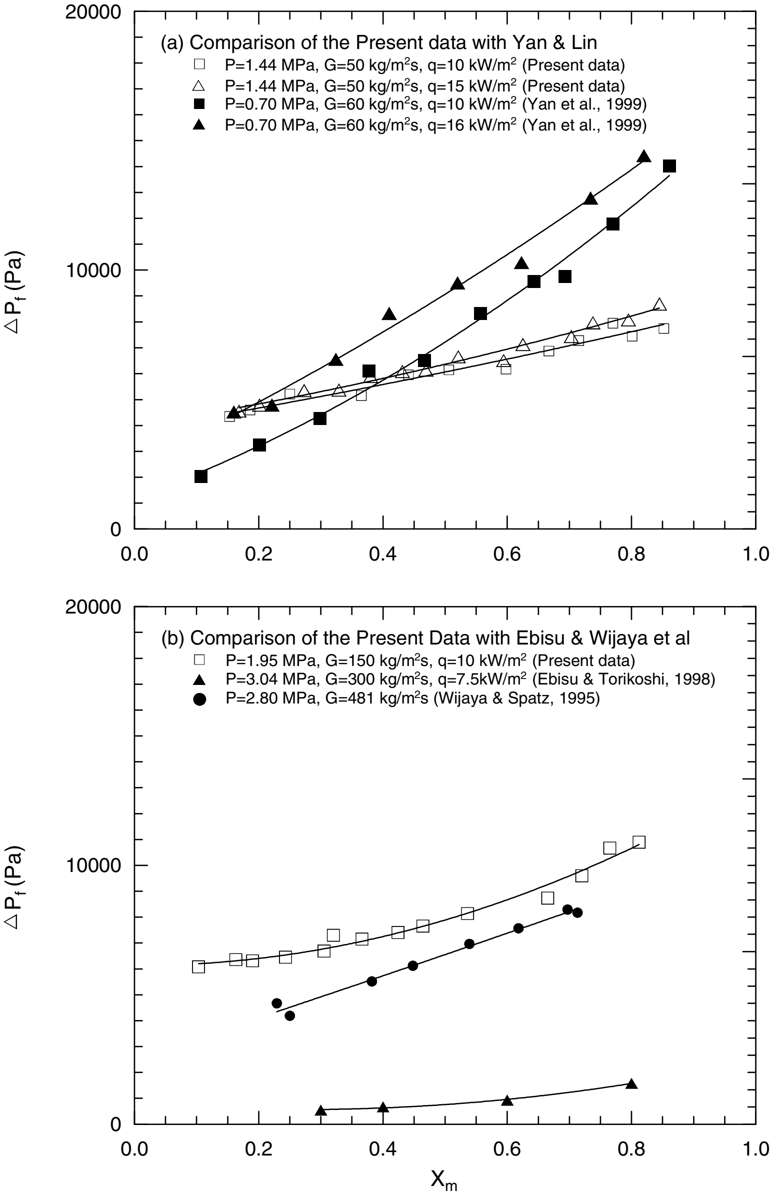

Fig. 8. Comparison of the measured frictional pressure drops for R-410A condensation in the PHE with those for (a) R-134a in the same PHE from Yan et al. (1999) and (b) R-410A in a horizontal smooth tube from Ebisu and Torikoshi (1998) and from Wijaya and Spatz (1995).

sure drop of R-410A in the plate heat exchanger is lower than that for R-134a in the same PHE, but it is much higher than that in a smooth horizontal pipe for the entire X_m range.

4.3. Correlation equations

According to the present data for R-410A condensation in the PHE, an empirical correlation for the condensation heat transfer coefficient is proposed, which is modified from that of Kandlikar [27]. The average condensation heat transfer coefficient is considered to be function of Convection, Froude and Boiling numbers. The proposed correlation for the R-410A condensation heat transfer coefficient is

$$h_r = h_{r,l} \cdot [0.25 \cdot Co^{-0.45} \cdot Fr_l^{0.25} + 75 \cdot Bo^{0.75}] \tag{16}$$

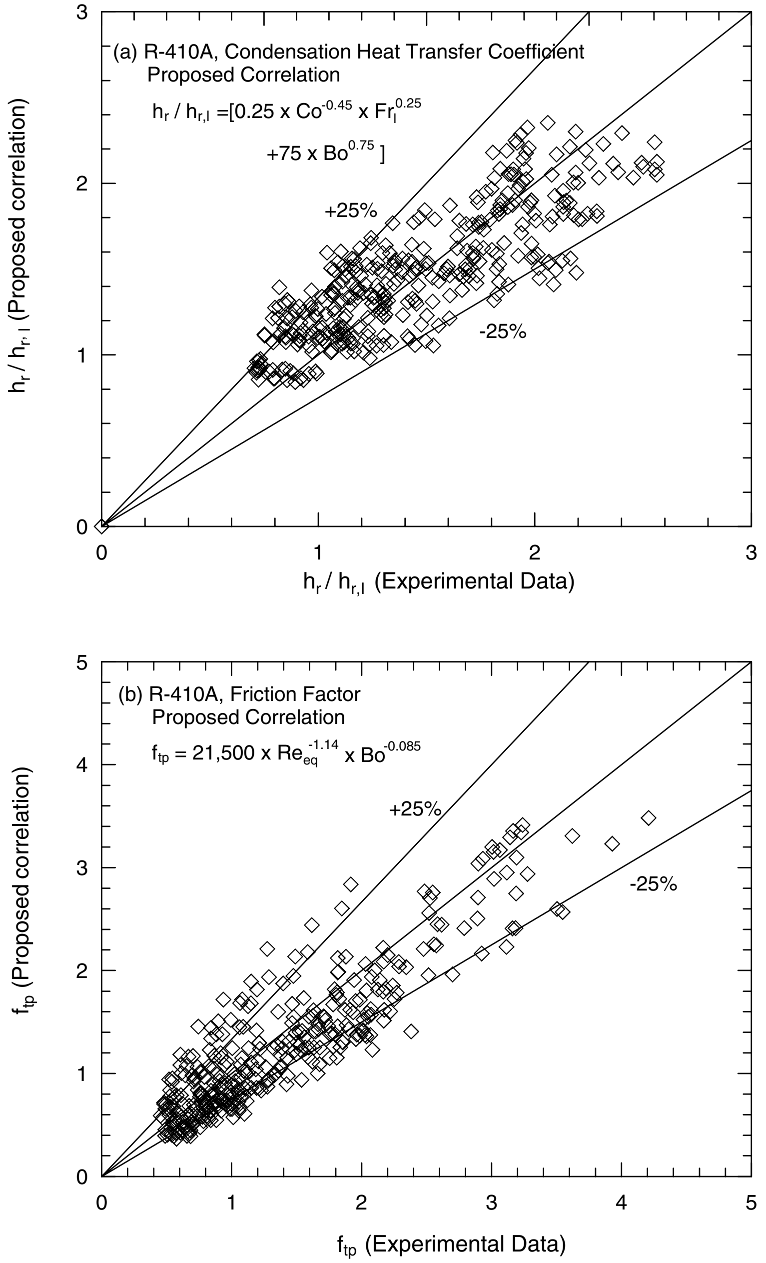

Fig. 9. Comparison of the proposed correlations with the present data for (a) condensation heat transfer coefficient and (b) friction factor.

and the data for the associated friction factor can be correlated as

$$f_{\mathrm{tp}} = 21,500 \cdot Re_{\mathrm{eq}}^{-1.14} \cdot Bo^{-0.085} \tag{17}$$

The single-phase convection heat transfer coefficient for liquid R-410A in this vertical plate heat exchanger has been established in our previous study [21] as

$$h_{\mathrm{r,l}} = 0.2092 \cdot \left(\frac{k_{\mathrm{l}}}{D_{\mathrm{h}}}\right) \cdot Re_{\mathrm{l}}^{0.78} \cdot Pr_{\mathrm{l}}^{1/3} \cdot \left(\frac{\mu_{\mathrm{ave}}}{\mu_{\mathrm{wall}}}\right)^{0.14} \tag{18}$$

In the above equations *Co*, *Fr*, *Bo* and *Pr* are respectively the Convection, Froude, Boiling and Prandtl numbers. They are respectively defined as

$$Co = \left(\frac{\rho_g}{\rho_l}\right) \cdot \left[\frac{(1 - X_m)}{X_m}\right]^{0.8} \tag{19}$$

$$Fr_l = \frac{G^2}{\rho_l^2 \cdot g \cdot D_h} \tag{20}$$

$$Bo = \frac{q}{G \cdot i_{fg}} \tag{21}$$

$$Pr_l = \frac{\mu_l \cdot c_{p,l}}{k_l} \tag{22}$$

and Re_{eq} is the equivalent Reynolds number regarding all the flow as liquid. Thus

$$Re_{eq} = \frac{G_{eq} \cdot D_h}{\mu_l} \tag{23}$$

in which

$$G_{eq} = G \cdot \left[(1 - X_m) + X_m \cdot \left(\frac{\rho_l}{\rho_g}\right)^{1/2}\right] \tag{24}$$

A data analysis shows that most of the present data are within 25% of deviations predicted from the above correlations (Fig. 9). More specifically, these correlation equations can represent our data with average deviations of 16% and 23% for the condensation heat transfer coefficient and friction factor, respectively.

5. Concluding remarks

We have measured the condensation heat transfer coefficient and frictional pressure drop of R-410A in a vertical plate heat exchanger. The effects of the refrigerant mass flux, imposed heat flux, system pressure and vapor quality on the measured data have been examined in detail. The major results can be summarized in the following.

(1) The heat transfer coefficient and associated frictional pressure drop for R-410A condensation in the PHE increase almost linearly with the mean vapor quality. But they are insensitive to the variation in the system pressure.
(2) Rises in the refrigerant mass flux and imposed heat flux result in better condensation heat transfer, accompanying with a larger pressure drop. Besides, the imposed heat flux exhibits stronger influences on the heat transfer coefficient and pressure drop than the refrigerant mass flux especially at low vapor quality.
(3) The effects of the refrigerant mass flux and vapor quality on the friction factor is rather significant, especially in the low vapor quality region. However, the imposed heat flux and refrigerant saturated pressure only slightly affect the friction factor.
(4) Correlation equations for condensation heat transfer coefficient and associated friction factor are proposed for R-410A flow in the PHE.

Acknowledgement

The financial support of this study by the engineering division of National Science Council of Taiwan, ROC through the contract NSC 85-2221-E-009-06 is greatly appreciated.

References

[1] P.A. Newman, Preserving earth's stratosphere, Mechanical Engineering 120 (1998) 88–91.
[2] S. Gopalnarayanan, Choosing the right refrigerant, Mechanical Engineering 120 (1998) 92–95.
[3] L.M. Schlager, M.B. Pate, A.E. Bergles, Heat transfer and pressure drop during evaporation and condensation of R-22 in horizontal micro-fin tubes, International Journal of Refrigeration 12 (1989) 6–14.
[4] L.M. Schlager, M.B. Pate, A.E. Bergles, Evaporation and condensation heat transfer and pressure drop in horizontal, 12.7-mm microfin tubes with refrigerant 22, ASME Journal of Heat Transfer 112 (1990) 1041–1047.
[5] X. Liu, Condensing and evaporating heat transfer and pressure drop characteristics of HFC-134a and HCFC-22, ASME Journal of Heat Transfer 119 (1997) 158–163.
[6] L.M. Chamra, R.L. Webb, Advanced micro-fin tubes for condensation, International Journal of Heat and Mass Transfer 39 (1996) 1839–1846.
[7] S.M. Sami, B. Poirier, Comparative study of heat transfer characteristics of new alternatives to R-22, ASHRAE Transactions 120 (1997) 824–829.
[8] T. Ebisu, K. Torikoshi, Heat transfer characteristics and correlations for R-410A flowing inside a horizontal smooth tube, ASHRAE Transactions 121 (1998) 556–561.
[9] H. Wijaya, M.W. Spatz, Two-phase flow heat transfer and pressure drop characteristics of R-22 and R-32/R125, ASHRAE Transactions 118 (1995) 1020–1027.
[10] A. Miyara, K. Nonaka, M. Taniguchi, Condensation heat transfer and flow pattern inside a herrigbone-type micro-fin tube, International Journal of Refrigeration 23 (2000) 141–152.
[11] M.S. Chitti, N.K. Anand, Condensation heat transfer inside smooth horizontal tube for R-22 and R-32/R-125 mixture, HVAC&R Research 2 (1996) 79–103.
[12] Z. Guo, N.K. Anand, Condensation of R-410A in a rectangular channel, HVAC&R Research 5 (1999) 99–123.
[13] Z. Guo, N.K. Anand, An analytical model to predict condensation of R-410A in a horizontal rectangular channel, ASME Journal of Heat Transfer 122 (2000) 613–626.
[14] R.K. Shah, W.W. Focke, Plate heat exchangers and their design theory, in: R.K. Shah, E.C. Subbarao, R.A. Mashelkar (Eds.), Heat Transfer Equipment Design, Hemisphere, Washington, DC, 1988, pp. 227–254.

[15] B. Thonon, R. Vidil, C. Marvillet, Recent research and developments in plate heat exchangers, Journal of Enhanced Heat Transfer 2 (1995) 149–155.

[16] C. Tribbe, H.M. Müller-Steinhagen, Gas/liquid flow in plate-and-frame heat exchangers—Part I: pressure drop measurements, Heat Transfer Engineering 22 (2001) 5–11.

[17] C. Tribbe, H.M. Müller-Steinhagen, Gas/liquid flow in plate-and-frame heat exchangers—Part II: Two-phase multiplier and flow pattern analysis, Heat Transfer Engineering 22 (2001) 12–21.

[18] G. Kreissig, H.M. Müller-Steinhagen, Frictional pressure drop for gas/liquid two-phase flow in plate heat exchangers, Heat Transfer Engineering 13 (1992) 42–52.

[19] Y.Y. Yan, T.F. Lin, Evaporation heat transfer and pressure drop of refrigerant R-134a in a plate heat exchanger, ASME Journal of Heat Transfer 121 (1999) 118–127.

[20] Y.Y. Yan, H.C. Lio, T.F. Lin, Condensation heat transfer and pressure drop of refrigerant R-134a in a plate heat exchanger, International Journal of Heat and Mass Transfer 42 (1999) 993–1006.

[21] Y.Y. Hsieh, T.F. Lin, Saturated flow boiling heat transfer and pressure drop of refrigerant R-410A in a vertical plate heat exchanger, International Journal of Heat and Mass Transfer 45 (2002) 1033–1044.

[22] Y.Y. Hsieh, L.J. Chiang, T.F. Lin, Subcooled flow boiling heat transfer of R-134a and the associated bubble characteristics in a vertical plate heat exchanger, International Journal of Heat and Mass Transfer 45 (2002) 1791–1806.

[23] Y.Y. Hsieh, T.F. Lin, Evaporative heat transfer and pressure drop of refrigerant R-410A flow in a vertical plate heat exchanger, ASME Journal of Heat Transfer 125 (2003) 852–857.

[24] E.E. Wilson, A basic for traditional design of heat transfer apparatus, ASME Journal of Heat Transfer 37 (1915) 47–70.

[25] S.J. Kline, F.A. McClintock, Describing uncertainties in single-sample experiments, Mechanical Engineering 75 (1) (1953) 3–12.

[26] J.G. Collier, Convective Boiling and Condensation, second ed., McGraw-Hill, 1982.

[27] S.G. Kandlikar, A general correlation for saturated two-phase flow boiling heat transfer inside horizontal and vertical tubes, ASME Journal of Heat Transfer 112 (1990) 219–228.